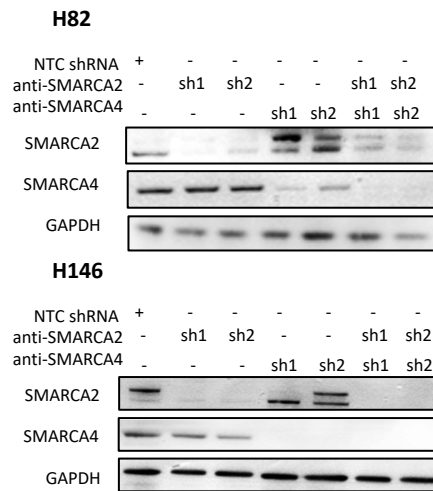


A

	CCLE			Rudin et al and George et al	
	Gene	r	p value	r	p value
NE	NCAM1	0.311	6.30E-08	0.67	<0.0001
	DLL3	0.43	2.47E-04	0.45	<0.0001
non-NE	NOTCH2	-0.393	7.25E-03	-0.1736	0.0491

B



C

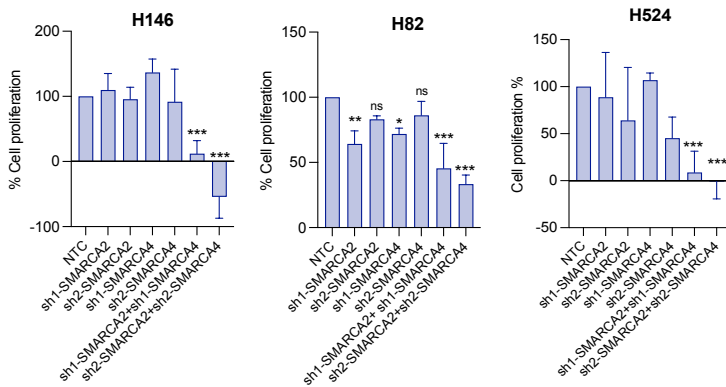
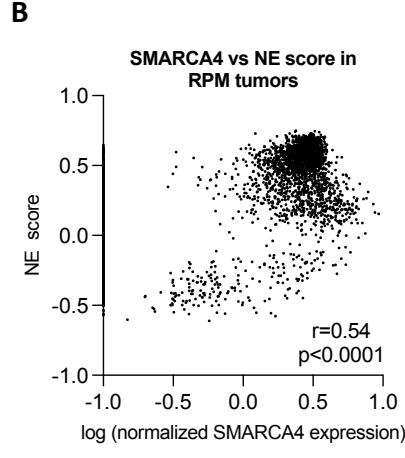
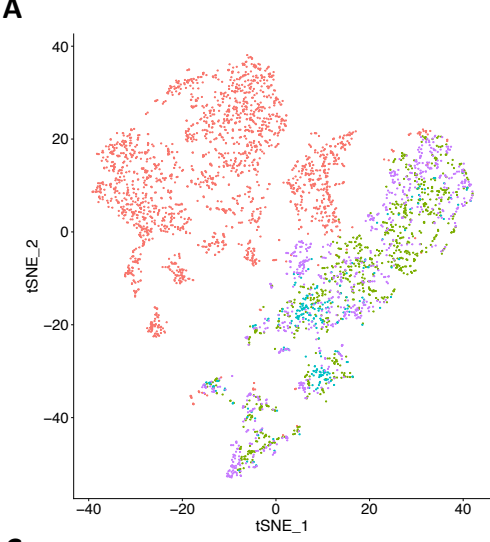


**Figure S1. Related to Fig. 1. *SMARCA4* expression correlates with NE markers and its inhibition together with *SMARCA2* KD decreases cell proliferation. A.** Spearman correlation of *SMARCA4* levels with *NCMA1*, *DLL3* and *NOTCH2*. **B.** Western blotting of *SMARCA4* and *SMARCA2* in isogenic cell lines derived from H82 and H146 cell lines expressing different combinations of short hairpin (sh) RNAs against *SMARCA4* and/or *SMARCA2*. **C.** Cell proliferation of genetic *SMARCA4* and/or *SMARCA2* knock-down cells at day 3. \* $p < 0.05$ , \*\*  $p < 0.01$ , \*\*\*  $p < 0.001$ .



**Figure S2. Related to Fig. 2. RNAseq in H82 and H146 cells treated with FHD-286 versus parental cells at day 14.** **A.** PCA plots of gene expression data from RNAseq performed in 3 or 4 biological replicates corresponding to untreated and FHD-286 treated H82 and H146 cells. **B.** Clustering of significant genes up- and downregulated upon treatment with FHD-286 imputed from RNAseq data (FDR $\leq$ 0.01, FC $>$ 1.5). **C.** *ASCL1* and *NEUROD1* gene expression levels (TPMs) in H146 (top) and H82 (bottom) cells determined by RNAseq. Student's two-tailed unpaired t test. \*\*p $<$ 0.01. **D.** Volcano plots showing preselected neuroendocrine and non-neuroendocrine genes that are significantly up- or downregulated upon treatment with FHD-286. See also Supplementary Table S1. **E.** IPA analysis on significantly downregulated genes (p $<$ 0.01) in FHD-286-treated cells versus untreated cells. **F.** GSEA analysis from data in Fig.2 showing enrichment in NOTCH and HIPPO/YAP1 pathways (FHD-286 treated vs untreated). **G.** Western blotting of neuroendocrine and non-neuroendocrine markers in NTC and sh-SMARCA4 and sh-SMARCA2 transduced cells at day 14.



Fisher analysis, p value<0.0001

	NE score>0	NE score<0
SMARCA4+	65%	14.5%
SMARCA4-	35%	85%
Total	100%	100%

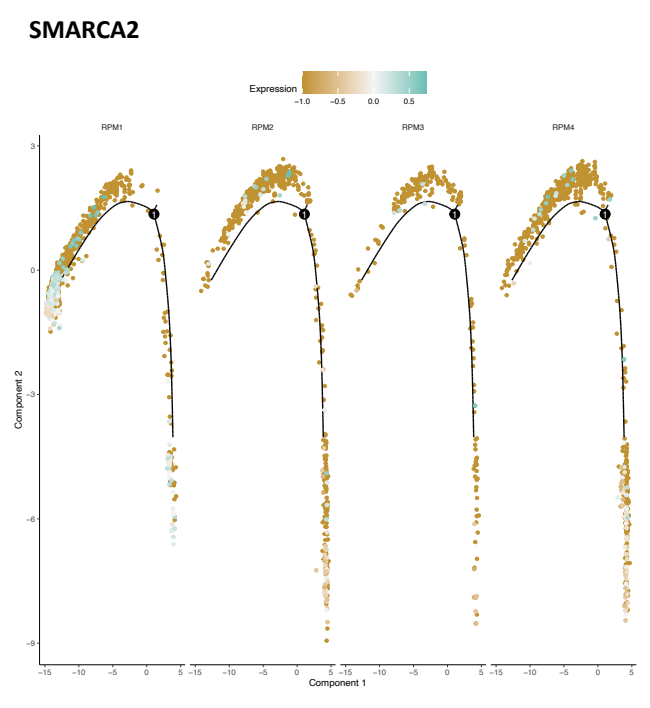
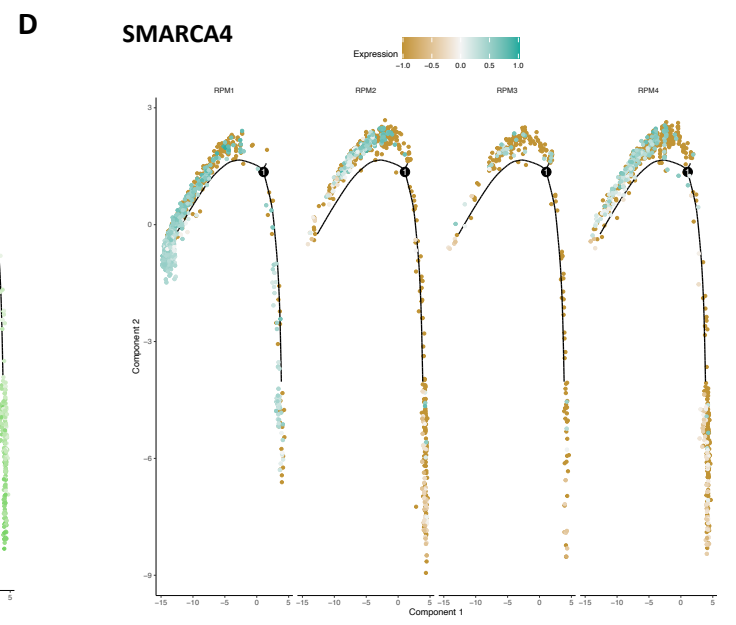
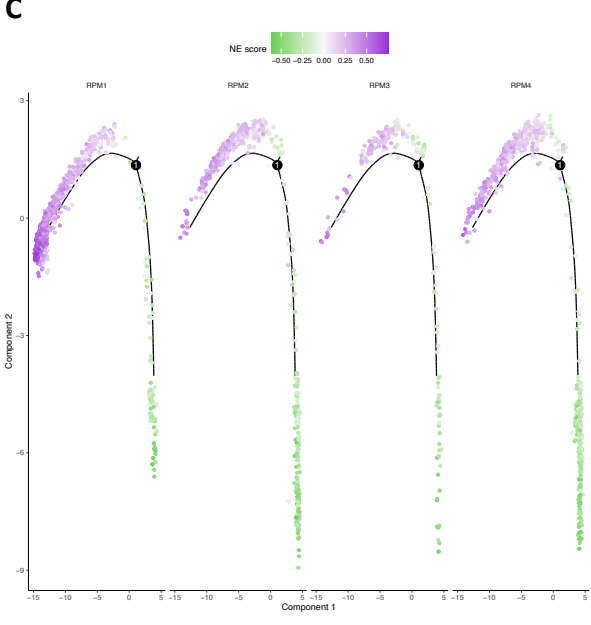




**Figure S3. Related to Fig.2. SMARCA4 correlates with a high NE score in a SCLC mouse model.** **A.** t-SNE plot of published scRNAseq data from 4 SCLC murine tumors from Ad-Cgrp-Cre-infected mice (6). **B.** Spearman correlation of Zhang NE score (28) and *SMARCA4* mRNA levels in Ireland et al (6). published scRNAseq data, and fisher analysis (two sided analysis) applied to these data. **C.** Expression of Zhang NE score projected onto pseudotime space in cells from (A). **D.** Pseudotime trajectory of *SMARCA4* and *SMARCA2* expression in the cells from (A).

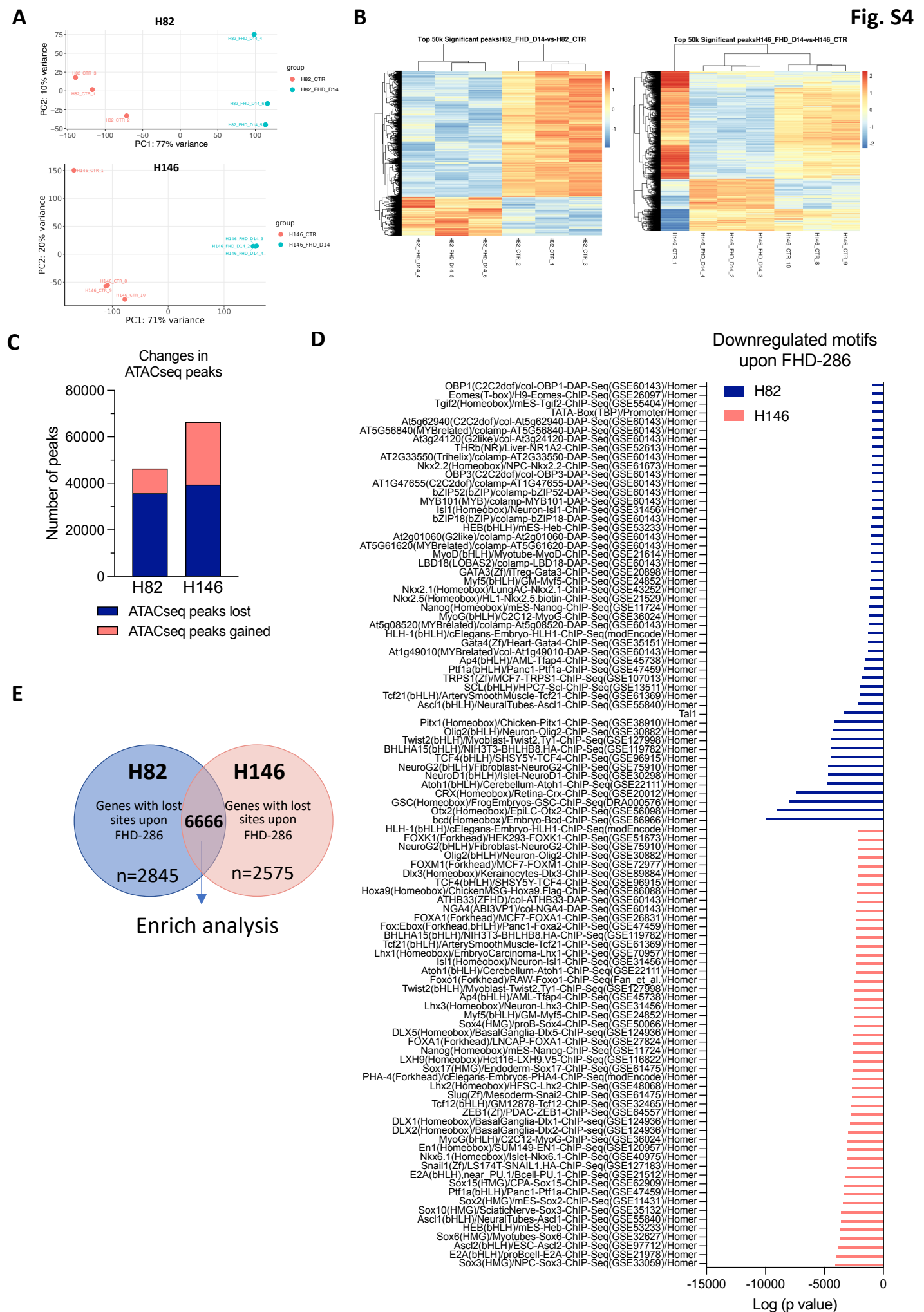


**Figure S4. Related to Figure 3. Pharmacological inhibition of SMARCA4 alters chromatin accessibility.** **A.** PCA plots of ATACseq data from 3 or 4 biological replicates corresponding to untreated and FHD-286 treated cells. **B.** Clustering of significant differentially ATACseq peaks upon treatment with FHD-286 (FDR $\leq$ 0.01, FC $>$ 1.5). **C.** Number of lost and gained sites in H82 and H146 cells after treatment with FHD-286 **D.** Top 50 HOMER motifs enriched at lost sites after SMARCA4/2 pharmacological inhibition. **E.** Venn diagram combining genes with lost sites upon FHD-286 treatment in both H146 and H82 cells. These common targets were used for the Enrich analysis in Fig. 3E. See also Table S2.

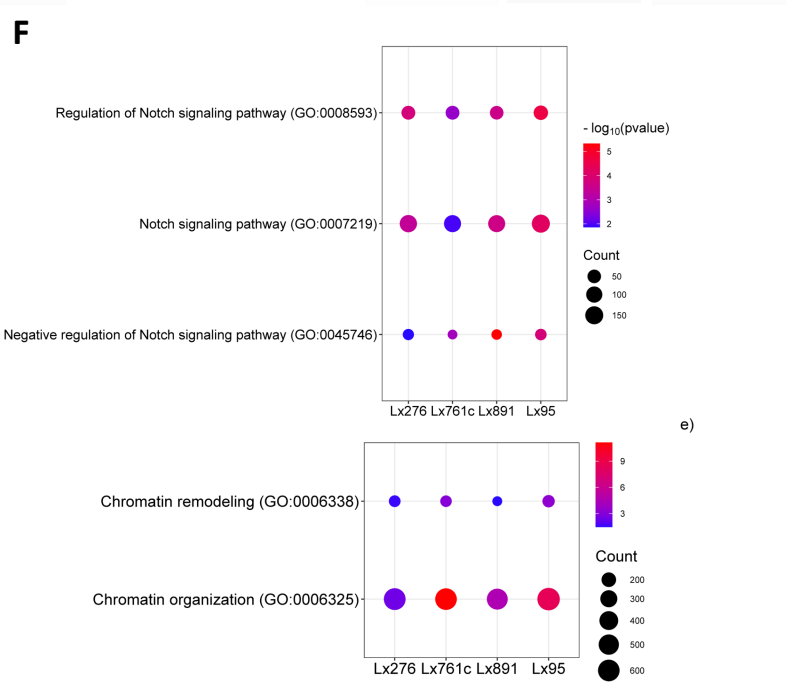
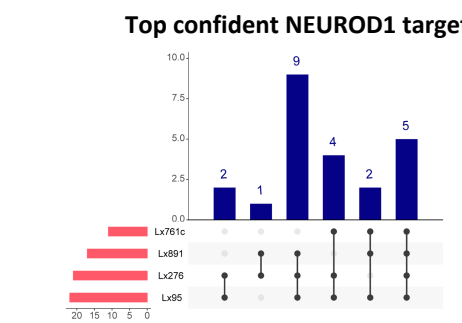
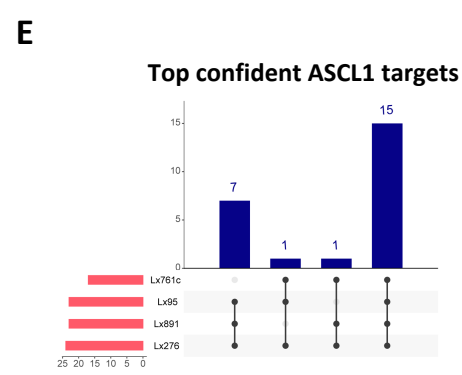
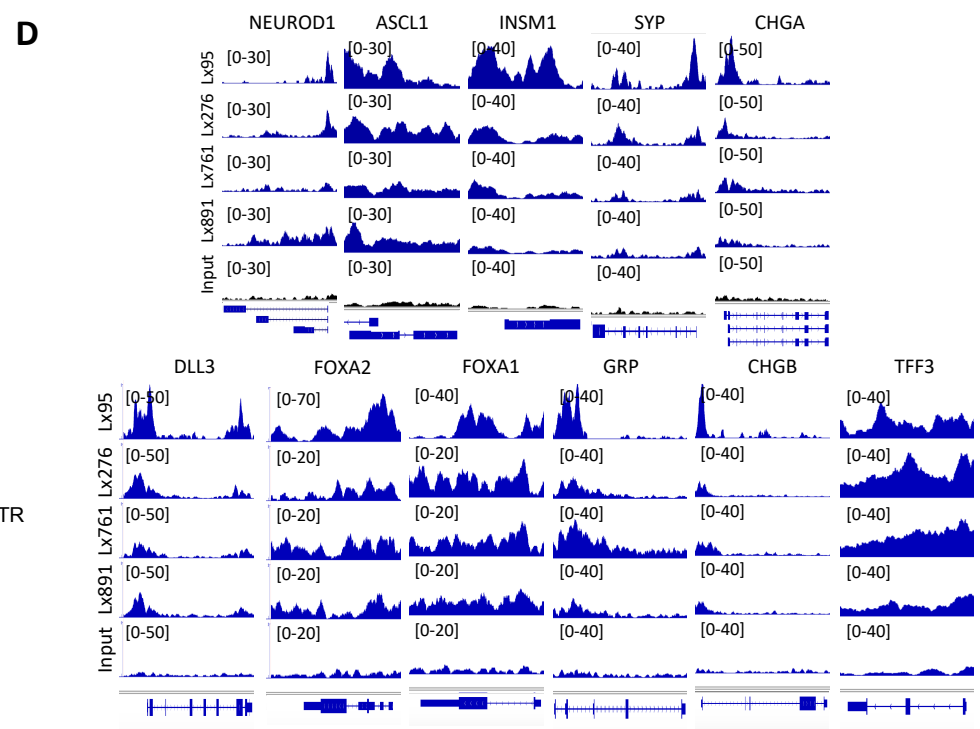
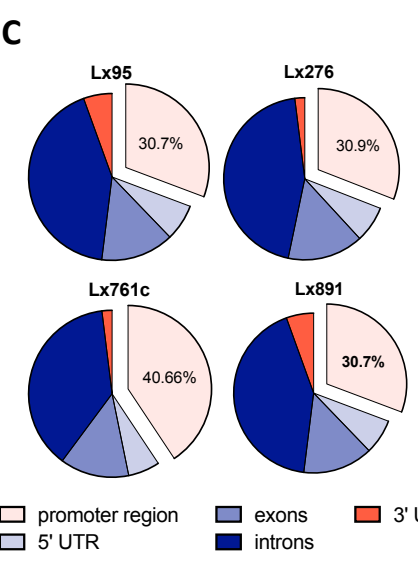
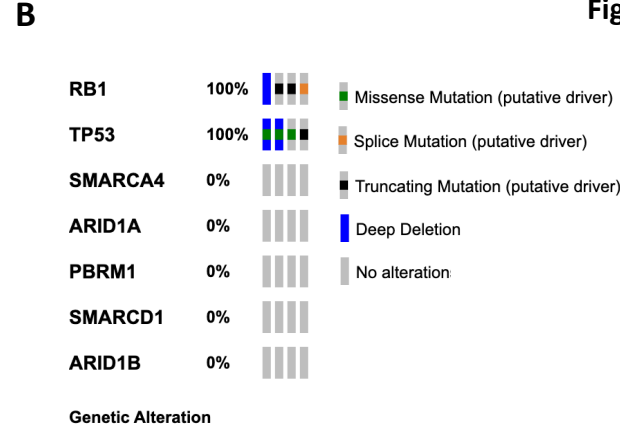
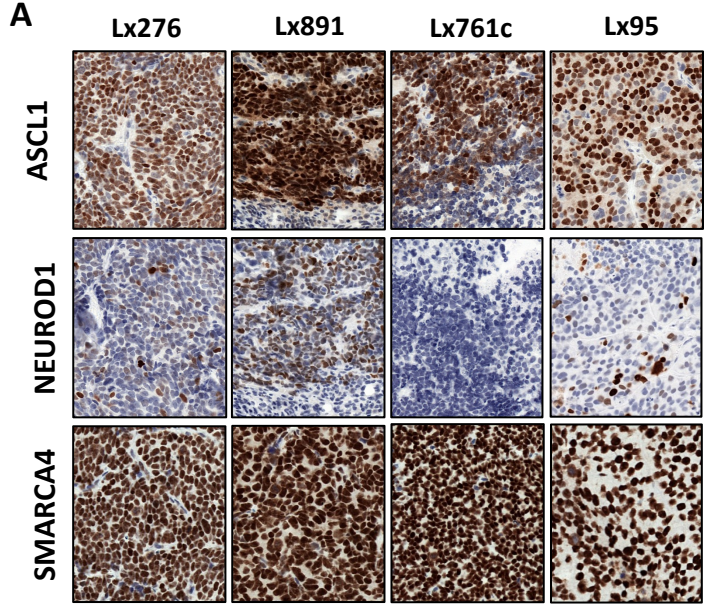


**Figure S5. Related to Fig. 4. SMARCA4 ChIP-seq binding profile.** **A.** IHC of ASCL1, NEUROD1 and SMARCA4 in the 4 NE SCLC PDXs used for SMARCA4 ChIP-seq. **B.** Oncoprint diagram of RB1, TP53, SMARCA4, ARIAD1A, PBRM1, SMARCAD1 and ARID1B determined by MSK-IMPACT in Lx276, Lx891, Lx761c and Lx95 (from left to right). **C.** Pie charts showing the percentage of SMARCA4 binding peaks at distinct genomic regions in the PDXs. **D.** Genome tracks of neuron and NE factors in SMARCA4 ChIP-seq data visualized with the Integrative Genomics Viewer (IGV)(34). **E.** Upset plots showing the number of ASCL1 and NEUROD1 confident targets overlapping with SMARCA4 targets identified in the ChIP-seq data. **F.** Dot plot of Poly-Enrich analysis performed to SMARCA4 ChIP-seq peaks. Pre-selected pathways related to NOTCH signaling and chromatin remodeling are shown. The counts refer to the number of genes detected in the ChIP-seq data that are part of the indicated pathways.

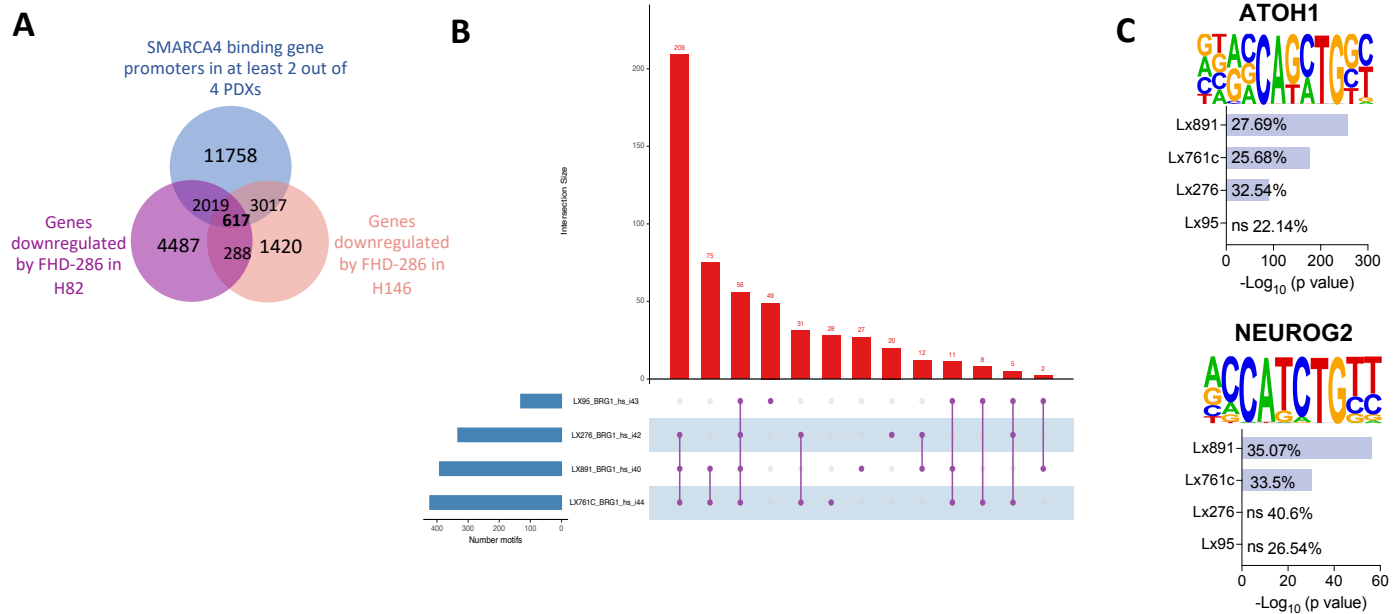


**Figure S6. Related to Fig. 4. SMARCA4 ChIP-seq binding profile.**

**A.** Venn diagram combining RNAseq data of H146 and H82 cells treated with FHD-286 versus untreated and SMARCA4 ChIP-seq peaks at promoter region in at least two out of the four PDXs characterized. **B.** Upset plot showing the abundance of common and unique SMARCA4 ChIP-seq enrichment motifs found in the 4 PDXs. **C.** Enrichment analysis of ATOH1 and NEUROG2 TF-binding motifs in the SMARCA4 ChIP-seq data identified with HOMER. See also Table S3.

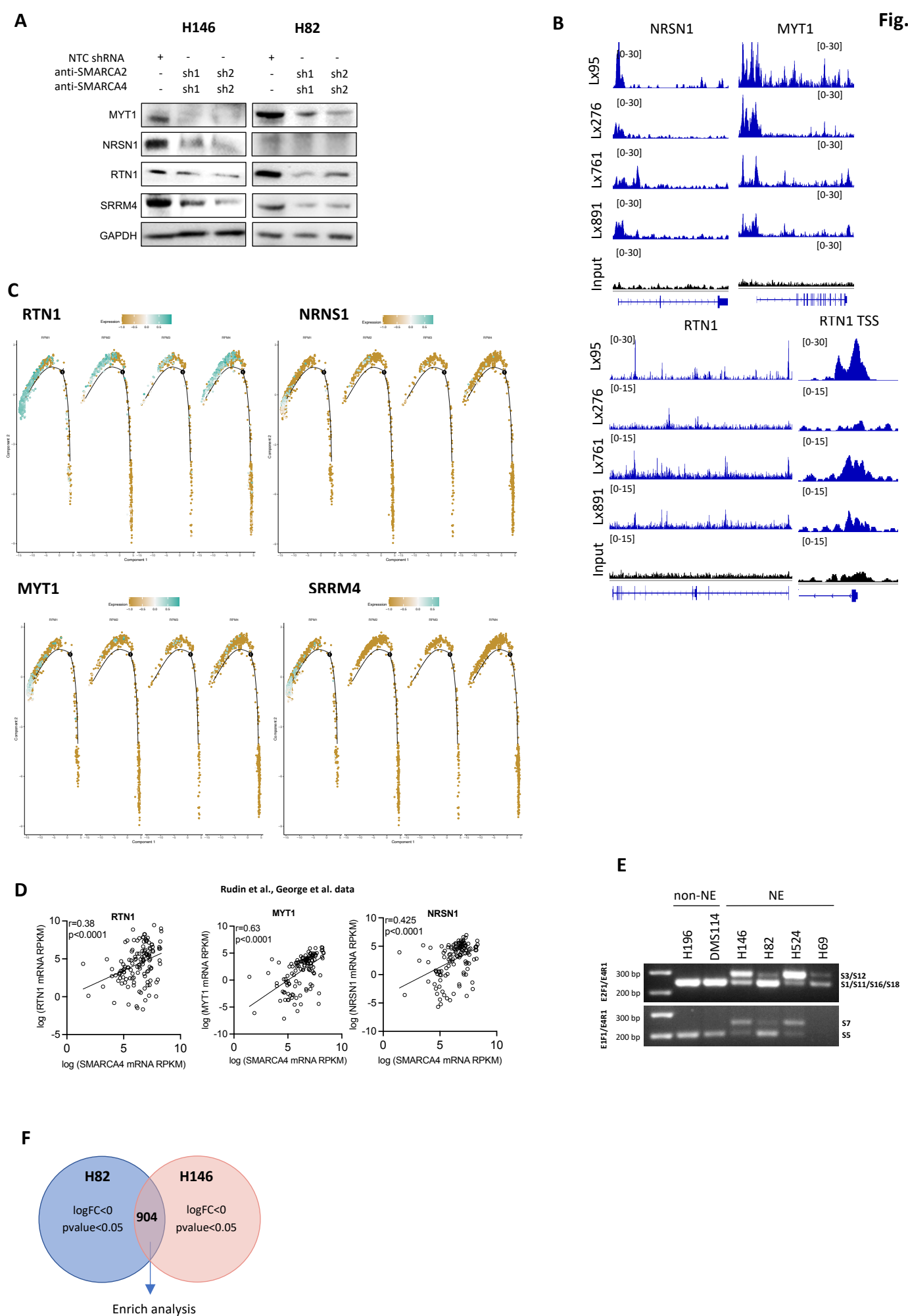


**Figure S7. Related to Fig.5. SMARCA4 regulates ASCL1 and NEUROD1 targets, and SRRM4 expression to control splicing and activation of REST. A.** Western blotting of *RTN1*, *NRSN1*, *MYT1* and *SRRM4* in NTC and in double knockdown *SMARCA4* and *SMARCA2* cells at day 14. **B.** Genome tracks of *NRSN1*, *MYT1*, *RTN1* retrieved from *SMARCA4* ChIP-seq data. Graphs were obtained from IGV (2.16.2)(34). **C.** Expression of *RTN1*, *NRSN1*, *MYT1* and *SRRM4* projected in a pseudotime trajectory from early to late time points in murine SCLC tumors from published scRNAseq (6). **D.** Spearman correlation of *RTN1*, *MYT1* and *NRSN1* with *SMARCA4* mRNA levels in Rudin et al (26). And George et al. (25) databases and CCLE. **E.** PCR analysis of REST splicing isoforms using two pairs of primers (E2F1+E4R1 and E1F1+E4R1) that span N3c in a panel with low and high NE phenotype. **F.** Venn diagram applied to genes significantly downregulated upon treatment with FHD-286 in the RNAseq (related to Fig. 5I). See also Table S1.



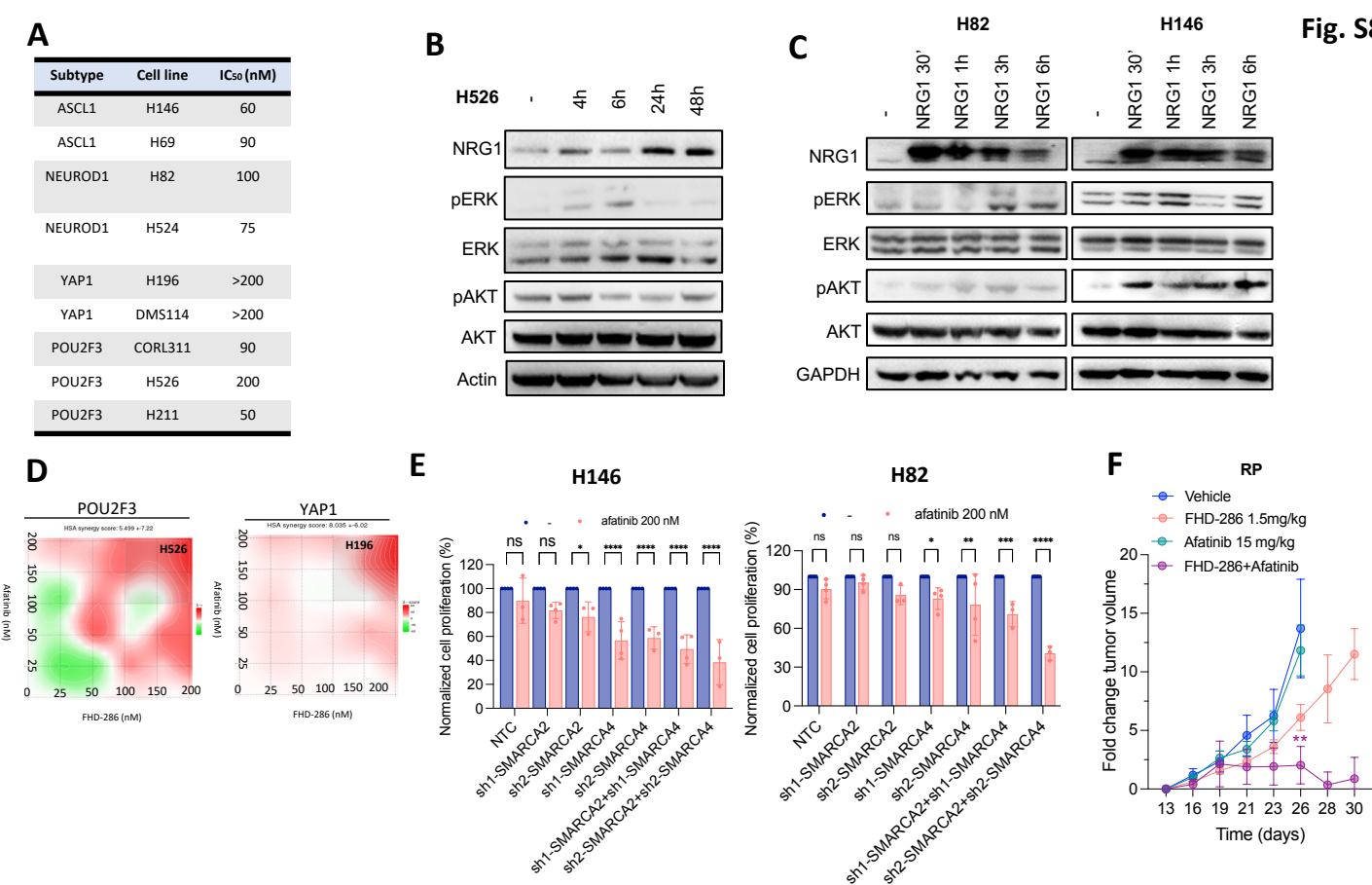


**Figure S8. Related to Fig. 6. A.** IC<sub>50</sub> for FHD-286 in SCLC-A, -N, -P and -Y SCLC cell lines treated at 96h. **B.** Immunoblot of ERBB family proteins in H526 cells after treatment with 100 nM of FHD-286 at the indicated times. **C.** Western blot in H82 and H146 cells treated with recombinant NRG1 (100ng/mL) at the indicated times. **D.** Synergy plots of FHD-286 and afatinib in non-NE SCLC cell lines. **E.** Normalized cell proliferation of sh-SMARCA2 and/or sh-SMARCA4 transduced cells after treatment with afatinib (200nM) for 72h. Data is shown as mean±SD. Student's two-tailed unpaired t test. \*p<0.05, \*\*\*p<0.001, \*\*\*\*p<0.0001. **F.** Normalized tumor growth of RP syngeneic cell line relative with respect to day 1 of treatment. Two-way ANOVA followed by Bonferroni comparison test. \*p<0.05, \*\*p<0.01, \*\*\*p<0.001.